Response of tropical Pacific interannual variability to decadal entrainment temperature change in a hybrid coupled model

Rong-Hua Zhang[1] and David G. DeWitt[2]

Received 21 November 2005; revised 21 March 2006; accepted 24 March 2006; published 29 April 2006.

[1] The role of decadal changes in ocean thermal structure, as observed in the tropical Pacific in the late 1970s, in modulating El Niño/Southern Oscillation (ENSO) is examined using a hybrid coupled model (HCM), consisting of an atmospheric general circulation model (AGCM; ECHAM4.5) and an intermediate ocean model (IOM) with an empirical parameterization for the temperature of subsurface water entrained into the mixed layer (T_e), which is constructed via a singular value decomposition (SVD) analysis of historical data. A standard HCM run produces irregularity of ENSO. Two perturbation runs are conduced by introducing the decadal changes in T_e estimated from two subperiods before and after the climate shift ($T_e^{63-79}$and T_e^{80-96}), respectively. Together with previous studies using an intermediate coupled model (ICM) consisting of the same IOM, different modulating effects of T_e in the ocean and stochastic forcing in the atmosphere are demonstrated on the properties of ENSO. The former is responsible for changes in the phase propagation of ENSO, while the latter can contribute to the amplitude and period modulation.
Citation: Zhang, R.-H., and D. G. DeWitt (2006), Response of tropical Pacific interannual variability to decadal entrainment temperature change in a hybrid coupled model, *Geophys. Res. Lett.*, *33*, L08611, doi:10.1029/2005GL025286.

1. Introduction

[2] Interannual variability in the tropical Pacific associated with ENSO has been observed to exhibit decadal changes in the late 1970s. For example, a westward phase propagation of SST anomalies along the equator is evident during the 1960s and 1970s. After the late 1970s, there is a clear tendency for SST anomalies to shift its propagation direction to be eastward. Great efforts have been devoted to understanding the decadal changes in ENSO [e.g., *Fedorov and Philander*, 2000; *Wang and An*, 2001]. For example, it has been demonstrated that stochastic forcing in the atmosphere can cause ENSO to be irregular in coupled models [e.g., *Kirtman and Schopf*, 1998; *Fluegel et al.*, 2004]. Significant changes in subsurface temperature structure were observed in the tropical Pacific Ocean in the late 1970s and their potential effects on ENSO variability have also been suggested [e.g., *Gu and Philander*, 1997; *Zhang et al.*, 1998]. At present, the exact mechanisms for decadal ENSO variability, such as whether it is an intrinsic tropical mode or induced extra-tropically, or whether the oceanic and/or atmospheric bridges connect the subtropics to the tropics, or it is forced randomly by atmospheric stochastic forcing and/or by deterministic processes still remain unresolved.

[3] *Zhang and Busalacchi* [2005] have identified T_e as a new factor in decadal ENSO variability using an ICM, demonstrating that the changes in subsurface ocean thermal structure, observed in the later 1970s, are able to modulate the ENSO properties. In this ICM, however, the atmospheric model is a statistical one, an empirical feedback response of wind stress to an SST anomaly that is estimated using an SVD of the covariance matrix. Atmospheric stochastic forcing, an important mechanism for being able to cause irregularity of ENSO, has not been taken into account.

[4] This paper continues to addresses the effect of decadal subsurface temperature changes on ENSO properties. Different from *Zhang and Busalacchi* [2005], a hybrid coupled model (HCM) consisting of a comprehensive AGCM is used, which introduces the AGCM as a source of stochastic forcing. The HCM simulations will be analyzed to examine the respective roles of atmospheric stochastic forcing and decadal T_e change in modulating ENSO properties.

2. Model Descriptions and Experiments

2.1. An Atmospheric GCM (AGCM) and an Intermediate Ocean Model (IOM)

[5] To examine the role of subsurface temperature in modulating ENSO properties in coupled tropical Pacific climate system, we develop an HCM combining the Max Planck Institute for Meteorology (MPI) ECHAM4.5 Atmospheric GCM (AGCM) [*Roeckner et al.*, 1996] and an IOM. The ECHAM4.5 AGCM is a global spectral model with triangular truncation at wavenumber 42 (T42). A complete description of the ECHAM4.5 is given by *Roeckner et al.* [1996]. The IOM was described by *Keenlyside and Kleeman* [2002] and *Zhang et al.* [2003]. The IOM's thermodynamics include an SST anomaly model with an empirical T_e parameterization, which is optimally calculated in terms of sea level (SL) anomalies using an SVD analysis from historical data [*Zhang et al.*, 2003].

2.2. Coupling Procedure

[6] The ECHAM4.5 is coupled to the IOM using the Ocean-Atmosphere-Sea Ice-Soil (OASIS) coupling software [*Terray et al.*, 1999] produced by the European Center for Research and Advanced Training in Scientific Computation (CERFACS). In the coupled integration, the AGCM provides anomalous momentum fluxes to the IOM. These anomalous fluxes are determined as the difference of the

[1]Earth System Science Interdisciplinary Center (ESSIC), University of Maryland, College Park, Maryland, USA.
[2]International Research Institute for Climate and Society (IRI), Earth Institute at Columbia University, Palisades, New York, USA.

0094-8276/06/2005GL025286$05.00

AGCM computed stress in the coupled run from the long term monthly mean climatology for the 1950–99 period that is obtained from a suite of 24 ensemble member AGCM stand alone runs made using observed SST. The IOM produces anomalous SL, mixed-layer averaged currents, vertical velocity at the based of the mixed layer (entrainment); T_e anomalies are estimated from the SL anomalies using the SVD technique, serving as an interface between the SST anomaly model and dynamical ocean model. SST anomalies are then determined using the simulated and prescribed oceanic fields (mean and anomaly currents). The resultant SST anomaly field is used to determine wind anomalies in the AGCM. Information between the AGCM and the IOM is exchanged once per day.

2.3. Numerical Experiments

[7] The decadal changes in subsurface temperature structure are taken into account in the following way using an empirical procedure [*Zhang and Busalacchi*, 2005]. Historical SL anomalies during the period 1962–1999 are obtained from the IOM run, forced by interannual wind stress anomalies from the NCEP-NCAR reanalysis [*Kalnay et al.*, 1996]. Historical T_e anomalies for the 1962–99 periods are estimated through an inverse procedure using oceanic fields simulated from the IOM and monthly SST fields observed by *Reynolds et al.* [2002]. An empirical relationship between the T_e and SL anomalies is constructed from the historical data. Thus, using the T_e model constructed, a given SL anomaly pattern can be converted into T_e anomalies, which are used in the SST calculation. A standard HCM run is performed using the T_e model constructed during the period 1963–96.

[8] Furthermore, two T_e models are constructed separately during two subperiods before (1963–79) and after (1980–96) the climate shift (T_e $^{63-79}$ and T_e $^{80-96}$), respectively. As shown in Figure 1, T_e shows large decadal changes in the late 1970s. In particular, after the late 1970s, T_e variability is substantially enhanced in the off-equatorial tropical North Pacific along 10°N between 140°E and the date line. As such, there can be significant differences in the intensity of estimated T_e anomalies from a given SL anomaly using T_e models constructed from these two subperiods.

[9] The T_e model constructed from each period is then specified for additional HCM simulations, with other aspects of the model setting keeping exactly the same. The effects of the decadal T_e changes on coupled behaviors can be examined in the context of the presence of atmospheric stochastic forcing in the HCM.

3. Simulated Interannual Variability

[10] A 41-year simulation is made using the HCM with the empirical T_e model constructed from the period 1963–96. The HCM produces significant interannual variability, characterized by irregularity of ENSO with a broad spectrum of periods between 2.4 year and 7.1 years. The simulated ENSO events show large changes in the amplitude and oscillation periods. Note that the previous ICM consisting of the same IOM [*Zhang and Busalacchi*, 2005] produces ENSO events that are quite regular, with a dominant 4 year oscillation period. This indicates that the presence of stochastic forcing in the atmosphere is contributing to the irregularity of the simulated ENSO in the HCM.

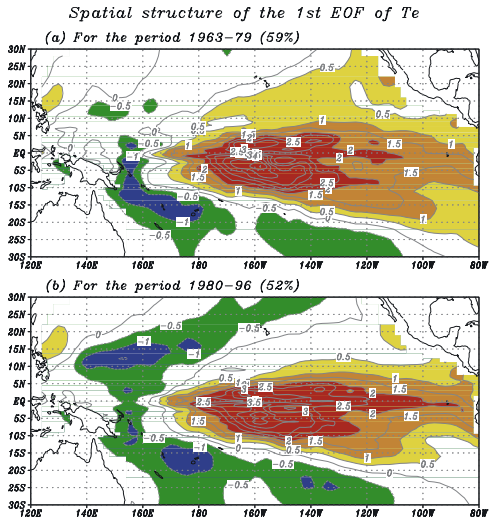

Figure 1. Spatial structures of the first EOF mode for T_e derived during the periods (a) 1963–79 and (b) 1980–96. The contour interval is 0.5.

[11] To demonstrate the effect of decadal subsurface temperature variability on coupled interannual variability in the HCM, two additional 23-year simulations are made using the T_e models constructed from two subperiods (T_e $^{63-79}$ and T_e $^{80-96}$). Figure 2 illustrates the longitude-time sections of SST anomalies along the equator from the two runs.

[12] In the T_e $^{63-79}$ run (Figure 2a), one striking feature is that the structure of simulated interannual variability is characterized by the predominance of westward propagation in SST and wind variations on the equator. Figure 3a presents time series of simulated SST anomalies in the Niño1+2 and the Niño3+4 regions, respectively. A clear phase lag in SST variations can be seen at the Niño3+4 site relative to those at the Niño1+2 site. So, SST anomalies can be seen to appear first in the eastern equatorial Pacific, then migrate westward along the equator. This is accompanied by wind anomalies which also show coherent westward propagation. When SST anomalies arrive in the central basin, large wind anomalies are induced in the central basin. Therefore, during an ENSO cycle, a phase propagation of coupled atmosphere-ocean anomalies is from the eastern basin to the central region along the equator. This coherent westward propagation feature is consistent with the development and evolution of composite anomalies associated with observed El Niño events during the 1950–73 periods.

[13] Superimposed on the westward propagation tendency is the irregularity of simulated ENSO events, with large changes in the amplitude and oscillation period (Figure 2a). To quantify the dominant time scales of the simulated interannual variability, power spectra are estimated from the Niño3 SST anomaly time series (Figure 4). There are mainly three statistically significant peaks with enhanced power, the first at 2.7 years, the second at 3.6 years and the third at 1.5 years, respectively.

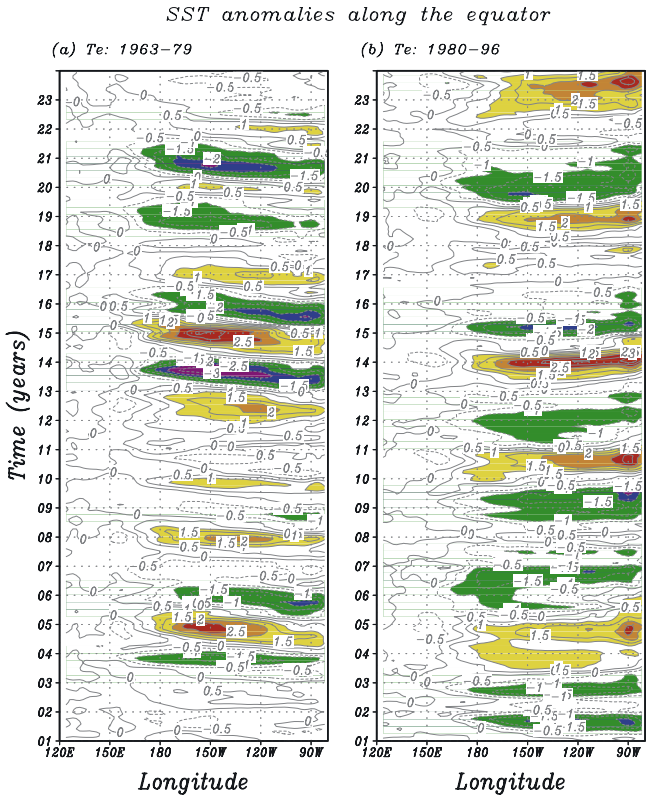

Figure 2. SST anomalies along the equator simulated in the HCM using the (a) T_e^{63-79} (b) and T_e^{80-96} models. The contour interval is 0.5 °C.

[14] In the T_e^{80-96} run (Figure 2b), the coupled interannual variability is characterized by an eastward propagation of SST anomalies on the equator. That is, SST anomalies first appear in the central basin near the date line, which are coupled with wind anomalies there which also progress eastward. In contrast to the T_e^{63-79} run (Figure 2a), a phase lead can be seen in the SST variations at the Niño3+4 site relative to the Niño1+2 site (Figure 3b). Thus the phase propagation of ENSO in the T_e^{80-96} run is eastward from the central basin to the eastern basin along the equator. In addition, as SST anomalies propagate eastward on the

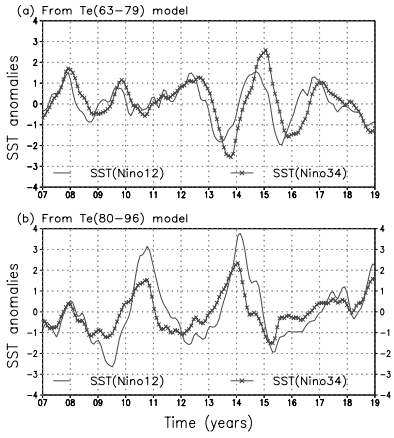

Figure 3. Monthly time series of the Niño-1+2 and Niño-3+4 SST anomalies in the HCM runs using the (a) T_e^{63-79} and (b) T_e^{80-96} models.

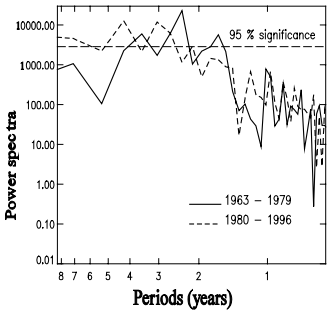

Figure 4. The spectra of the Niño3 SST anomalies simulated in the HCM runs using the T_e^{63-79} (solid line) and T_e^{80-96} (dashed line) models, respectively.

equator, they get amplified so that the largest SST anomalies are located in the far eastern equatorial Pacific (Figure 2b). The estimated spectra of SST anomalies (Figure 4) at the Niño3 site in the T_e^{80-96} run show a clear shift toward lower frequency side; the two statistically significant power peaks are at 5.6 years (the first peak) and at 2.7 years (the second peak), respectively.

[15] As shown in Figure 1, thermal structure in the tropical Pacific exhibits decadal changes that took place in the late 1970s. As a result, important differences exist in the spatial structure and amplitude of T_e anomalies estimated from the two subperiods 1963–1979 and 1980–1996, respectively. During the former period, T_e variability is relatively weak both in the eastern equatorial Pacific and in the off-equatorial tropical North Pacific near the date line. So, the influence of the zonal advection is more dominant in the SST budget, causing SST anomalies to propagate westward. After the late 1970s, the thermocline had been shoaling in the western tropical Pacific (but deepening in the east); the surface ocean mixed layer was also relatively shallow in the western and central tropical Pacific, particularly off the equator in the north. As a result, larger T_e anomalies are present in the eastern equatorial Pacific, which promotes the influence of the vertical advection on SST variability through the Bjerknes feedback. Moreover, a pronounced T_e anomaly center is located in the off-equatorial tropical North Pacific (around 10°N) between 140 °E and the date line (Figure 1b). As a result, subsurface anomalies can more easily get exposed to the surface in the off-equatorial tropical North Pacific near the date line. In fact, in the T_e^{80-96} run, an SST anomaly can be seen to form *first* in the central basin near the date line, induced by an T_e anomaly. So, an ENSO oscillation gets started first in the central basin and then propagates eastward along the equator as observed for ENSO evolution since the late 1970s.

[16] A brief comparison can be made between the simulated interannual variability using the ICM given by *Zhang and Busalacchi* [2005] and HCM described here. The simulated ENSO in the HCM is randomly irregular as manifested in the amplitude and oscillation periods (Figure 2), whereas it is very regular in the ICM simulation [*Zhang and Busalacchi*, 2005]. This indicates that stochastic forcing in the atmosphere is contributing to the irregularity of ENSO amplitude and oscillation period in the HCM simulations. However, during ENSO cycles, regardless of

atmosphere models used in these coupled ICM and HCM simulations, SST anomalies always display westward propagation when using the T_e^{63-79} model, but eastward when using the T_e^{80-96} model. This indicates that atmospheric stochastic forcing can randomly contribute to the amplitude and period modulation, but has not caused a regime shift in the phase propagation. Our modeling evidence suggests that during ENSO cycles, the phase initiation site and its subsequent propagation direction is modulated by T_e.

4. Discussions

[17] In this paper, a hybrid coupled model (HCM), consisting of a comprehensive AGCM and an intermediate complexity ocean model, is used to examine the sensitivity of ENSO properties to decadal changes in the structure of subsurface temperature in the tropical Pacific. The decadal changes in upper-ocean temperature observed in the late 1970s are incorporated into the coupled model via an empirical T_e parameterization which is constructed from two subperiods corresponding to the pre- and post-climate shift. Different T_e specifications in the HCM can have significant effects on the simulated interanuual variability characteristics. The manners in which ENSO events evolve and the phase relationships among atmosphere-ocean anomalies are strikingly different. Together with previous studies using an ICM consisting of the same IOM, different modulating effects of T_e in the ocean and stochastic forcing in the atmosphere are demonstrated on the properties of ENSO. Random atmospheric disturbances can make ENSO irregular in terms of the amplitude and oscillation period, while the changes in subsurface thermal structure is likely responsible for the shift in phase propagation of ENSO. The changes in the T_e specifications from the pre-climate to post-climate shift periods cause the ENSO modulation, which is consistent with what was observed in the late 1970s.

[18] **Acknowledgments.** We would like to thank A. J. Busalacchi and S. E. Zebiak for their comments, and J. Ballabrera-Poy for plotting figures. The authors wish to thank anonymous reviewers for their comments. This research is supported by NASA Grant NAG512246 for funding of the Pacific Subtropical Cells (Zhang) and by NOAA grant/cooperative agreement (NA07-GP0213; DeWitt).

References

Fedorov, A. V., and S. G. H. Philander (2000), Is El Niño changing?, *Science*, *228*, 1997–2002.

Fluegel, M., P. Chang, and C. Penland (2004), The role of stochastic forcing in modulating ENSO predictability, *J. Clim.*, *17*, 3125–3140.

Gu, D.-F., and S. G. H. Philander (1997), Interdecadal climate fluctuations that depend on exchanges between the tropical and extratropics, *Science*, *275*, 805–807.

Kalnay, E., et al. (1996), The NMC/NCAR reanalysis project, *Bull. Am. Meteorol. Soc.*, *77*, 437–471.

Keenlyside, N., and R. Kleeman (2002), Annual cycle of equatorial zonal currents in the Pacific, *J. Geophys. Res.*, *107*(C8), 3093, doi:10.1029/2000JC000711.

Kirtman, B. P., and P. S. Schopf (1998), Decadal variability in ENSO predictability and prediction, *J. Clim.*, *11*, 2804–2822.

Reynolds, R. W., N. A. Rayner, T. M. Smith, D. C. Stokes, and W. Wang (2002), An improved in-situ and satellite SST analysis for climate, *J. Clim.*, *15*, 1609–1625.

Roeckner, E., et al. (1996), The atmospheric general circulation model ECHAM-4: Model description and simulation of present-day climate, *Technical Report 218*, 90 pp., Max-Planck Inst. for Meteorol., Hamburg, Germany.

Terray, L., A. Piacentini, and S. Valcke (1999), OASIS 2.3, Ocean atmosphere sea ice soil: User's guide, *CERFACS Tech. Rep. TR/CMGC/99/37*, 82 pp., Cent. Eur. de Rech. et de Form. Avancée en Calcul Sci., Toulouse, France.

Wang, B., and S.-I. An (2001), Why the properties of El Niño changed during the late 1970s, *Geophys. Res. Lett.*, *28*(19), 3709–3712.

Zhang, R.-H., S. E. Zebiak, R. Kleeman, and N. Keenlyside (2003), A new intermediate coupled model for El Niño simulation and prediction, *Geophys. Res. Lett.*, *30*(19), 2012, doi:10.1029/2003GL018010.

Zhang, R.-H., and A. J. Busalacchi (2005), Interdecadal changes in properties of El Niño in an intermediate coupled model, *J. Clim.*, *18*, 1369–1380.

Zhang, R.-H., L. M. Rothstein, and A. J. Busalacchi (1998), Origin of upper-ocean warming and El Niño change on decadal scale in the tropical Pacific Ocean, *Nature*, *391*, 879–883.

D. G. DeWitt, International Research Institute for Climate and Society (IRI), Earth Institute at Columbia University, 61 Route 9W, Monell Building, Palisades, NY 10964–8000, USA.

R.-H. Zhang, Earth System Science Interdisciplinary Center (ESSIC), University of Maryland, 2207 Computer and Space Science Building, College Park, MD 20742–2465, USA. (rzhang@essic.umd.edu)

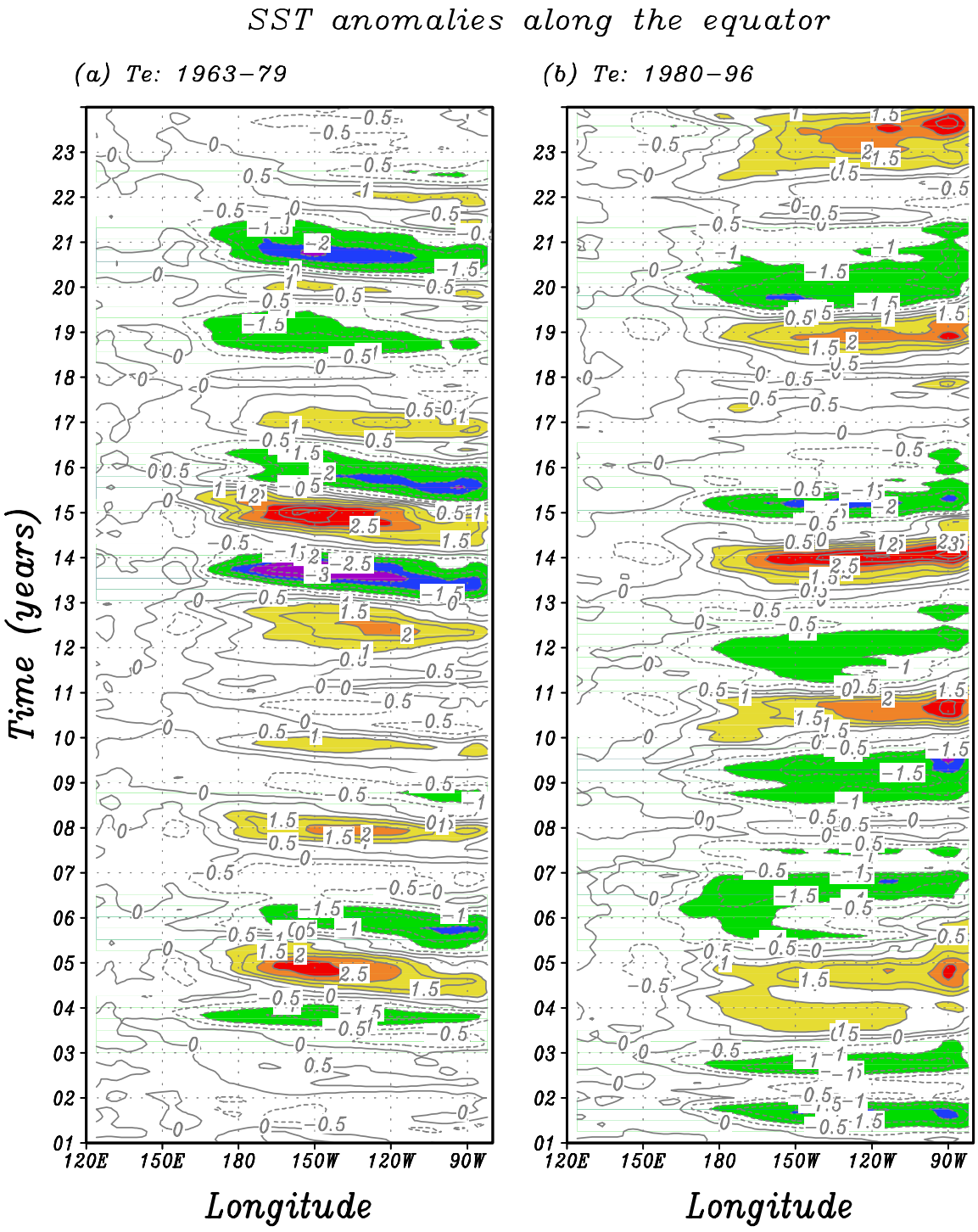

Fig. 2 SST anomalies along the equator simulated in the HCM using the $T_e^{63\text{-}79}$ (a) and $T_e^{80\text{-}96}$ (b) models, respectively. The contour interval is 0.5 °C.